IEEE Access
Multidisciplinary | Rapid Review | Open Access Journal

Received July 15, 2021, accepted August 6, 2021, date of publication August 17, 2021, date of current version August 27, 2021.

Digital Object Identifier 10.1109/ACCESS.2021.3105412

Stabilized Inertial Guidance Solution for Rolling Projectile Based on Partial Strapdown Platform

XIAO-MIN DUAN[1] AND HUILIANG CAO[2], (Member, IEEE)
[1]School of Electronic Science and Engineering, University of Electronic Science and Technology of China, Chengdu 610054, China
[2]Science and Technology on Electronic Test and Measurement Laboratory, North University of China, Taiyuan 030051, China

Corresponding author: Huiliang Cao (caohuiliang@nuc.edu.cn)

This work was supported in part by the National Natural Science Foundation of China under Grant 51705477, in part by the Aeronautical Science Foundation of China under Grant 2019080U0002, in part by the Fund of Key Research and Development (R&D) Projects of Shanxi Province under Grant 202003D111004, and in part by the Fund for Shanxi "1331 Project" Key Subjects Construction.

ABSTRACT It is extremely challenging to apply an Inertial Navigation System (INS) to a gun-launched rolling projectile effectively. Overcoming the negative effects produced by high angular rolling and over-loading requires innovative solutions. This paper introduces a unique inertial system that differs from a traditional gimballed INS and a strapdown INS. A Partial Strapdown Platform (PSP) was developed based on the principle of a pendulum to mitigate the adverse effects of projectile rolling motion. The anti-overloading performance of the PSP was improved by using a pair of specially designed alloy steel head-on hemispheres. Force condition analysis was conducted on the projectile and the PSP's inner cylinder to establish the mechanical dynamic model. Computer simulations and turntable experiments were performed to verify the stabilization function of the PSP. The pitch angle was determined to be associated with the stability of the PSP based on simulations and experiments. Gun firing tests were performed to verify the overload-burdening and stabilization functions of the PSP.

INDEX TERMS Inertial navigation, guided projectile, partial strapdown, mechanical dynamic.

I. INTRODUCTION

An Inertial Navigation System (INS) has many advantages, such as complete independent functioning, not being easily disturbed, and capturing of complete navigation data [1], [2], but it does not play a more significant role in the functioning of a projectile [3]. One main issue that large shocks and vibrations are encountered during the launch [4]. The other more important issue is that the projectile usually remains at a very high rotation speed during flight [5].

Projectiles are characterized by a small-caliber, low cost, high-speed rotation, and huge launching over-loading [6], [7]. Therefore, applying the gimballed INS, characterized by the large volume, high cost, and poor anti-overload performance, to a projectile is difficult. Likewise, a high projectile spin rate causes a complete strapdown system to exhibit a critical roll error sensitivity to scale factor uncertainty, making the strapdown INS also unsuitable for use on a projectile [8].

Studies of inertial projectile guidance are found in the literature. The navigational concepts in these papers include an integrated Global Positioning System (GPS)/INS, a gyroscope-free strapdown INS coupled with magnetic sensors, and a servomotor stable system [9]–[13]. These strategies are considered suitable for applications with different kinds of projectiles.

A miniature rugged integrated GPS/INS has been applied in short-range, slow-rolling rockets and missiles [14]. An air-to-surface tactical missile named the High-Speed Anti-Radiation Missile (HARM) has received a GPS/INS upgrade that improves its effectiveness and minimizes friendly-fire accidents [15]. An approach to enhance the performance of tightly coupled GPS/INS integration for missile applications has been introduced by [16].

A gyroscope-free strapdown INS has been applied in gun-launched rolling projectiles [17]. This system was considered to have excellent anti-overloading performance. Nevertheless, the disadvantage of the gyroscope-free system is that it has a low accuracy of measurement. The use of integrated magnetic sensors with the gyroscope-free strapdown INS could improve the precision to some extent. Nevertheless, the magnetic signals have easily been jammed on many occasions. The Autonomous Naval Support Round (ANSR) gun-launched guided projectile employs a strapdown inertial measurement unit composed of six

The associate editor coordinating the review of this manuscript and approving it for publication was Chunsheng Zhu.

This work is licensed under a Creative Commons Attribution 4.0 License. For more information, see https://creativecommons.org/licenses/by/4.0/

Commercial-Off-The-Shelf (COTS) accelerometers and a single three-axis magnetometer in work [18]. Reference [19] has researched the integrated navigation method with IMU and a magnetic sensor for situations that involve shock and high-speed rolling.

Some high-rolling, low-launch overload, small-caliber rockets, and missiles have adopted inertial guidance with a stable servomotor system. Such a system can isolate the Inertial Measurement Unit (IMU) from the rolling motion of the rocket but always has poor anti-overloading performance. The relevant literature has been previously discussed. Work [20] introduced a miniature roll-stabilized inertial measurement system that used a servomotor to stabilize the roll axis; this system survived a 40 g acceleration test. The anti-ship missile Penguin Mk3 is equipped with an INS platform that uses a servomotor spinning in the opposite direction to counterbalance the rotation of the missile; this system can withstand an overload of 100 g.

This paper presents a low-cost anti-overloading stabilized platform solution to projectile inertial guidance, the Partial Strapdown INS (PSINS). It is expected to be more applicable in high-speed rotation situations than the integrated GPS/INS, have higher accuracy than the gyroscope-free strapdown INS and have better anti-overloading than the servomotor stable method. This solution utilizes a Partial Strapdown Platform (PSP) to isolate the INS from the rolling motion of the projectile. Mechanical analysis and model simplification of the PSP were carried out. A dynamics model of the PSP's inner cylinder was built and calculated. Computer simulations were performed to analyze the stability of the PSP's inner cylinder. Turntable tests were performed to verify the computer simulation results. Gun firing tests were used to verify the overload-burdening and stabilization functions of the PSP. Note that the PSP is a despinning part of the projectile and that this will result in instability of the projectile in flight [21]–[26]. In work [27], the installation axial angle errors of semi-strap down IMS were analyzed and compensated. The experimental simulation results show that the method effectively reduces the periodic attitude measuring error caused by installation axial angle errors to 0.05° from 0.32°. A semi-strapdown stabilization platform is introduced and tested under a lab environment in work [28], and the ''counter-top hemisphere'' structure was employed, which play an influential protective role when 11 000g shock was input. However, this was not discussed in detail because this study focused on the relative stability between the inner cylinder of the PSP and the projectile in the spin axis.

This paper focuses on the width pulse and high G shock shooting range experiment based on the accurate artillery, and the rest of the paper is organized as follows: an explanation of the composition of the PSINS is given, followed by a description of the basic structure of the PSP. Then, mechanical analyses and dynamic modeling of the PSP's inner cylinder are described, and computer simulations and turntable experiments to verify the stability of the PSP are reported. Finally, gun firing tests supporting the anti-overloading performance and stabilization functions of the PSP are presented.

II. COMPOSITION OF PSINS

The PSINS is typically composed of an IMU, a photoelectric encoder, a slip ring, and a digital signal processor (DSP) circuit. The PSP's function is to provide a stable platform to separate the IMU from the projectile rolling motion. The IMU was installed in the PSP's inner cylinder to conduct attitude and position measurements. The photoelectric encoder was used to measure the relative rotating speed between the PSP's inner cylinder and the projectile. The projectile's initial attitude and position information and the inner cylinder's angle information in the roll axis should be loaded in the initial alignment stage. When establishing the attitude matrix, information concerning the output of the three orthogonal gyroscopes and the relative rotation speed is necessary. The working principle of the PSINS is shown in Figure 1.

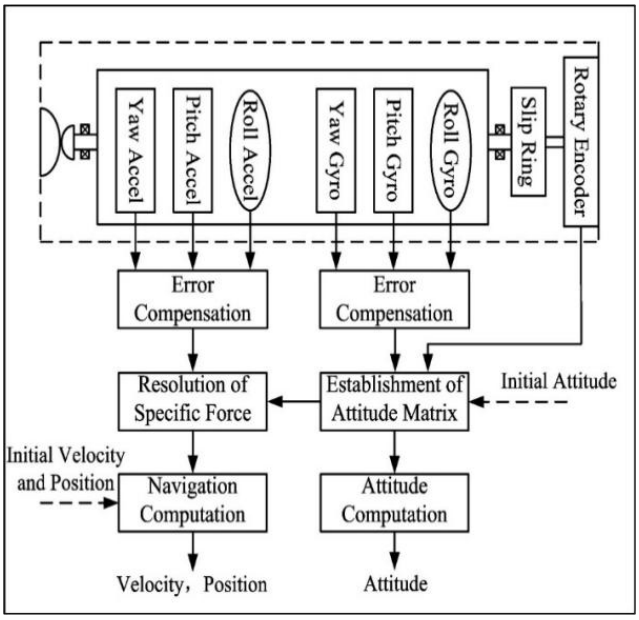

FIGURE 1. Block diagram showing working principle of PSINS.

III. PSP STRUCTURE

The PSP was designed based on the principle of a single pendulum motion. As shown in Figure 2, the pendulum extends vertically downward by the force of gravity, and it is stabilized at an equilibrium position until affected by an external force. When there is an external force, the pendulum leaves its fixed position, and gravity will concurrently provide the pendulum with a restoring moment, which will lead the pendulum to move towards its fixed position.

The PSP structure is as shown in Figure 3. A pair of deep groove ball bearings support an alloy steel inner cylinder. The centroid position of the inner cylinder is below its axis. The inner cylinder and bearing form a compound pendulum. The IMU and DSP circuit is installed in the inner cylinder.

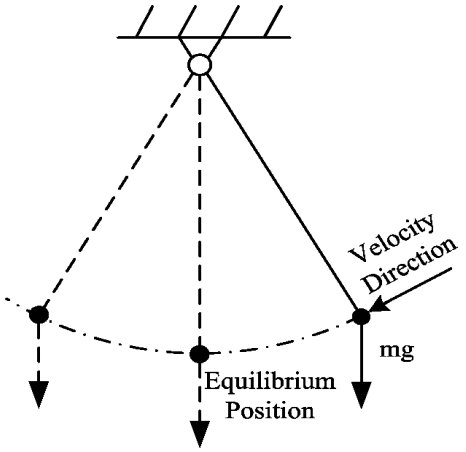

FIGURE 2. Schematic of pendulum.

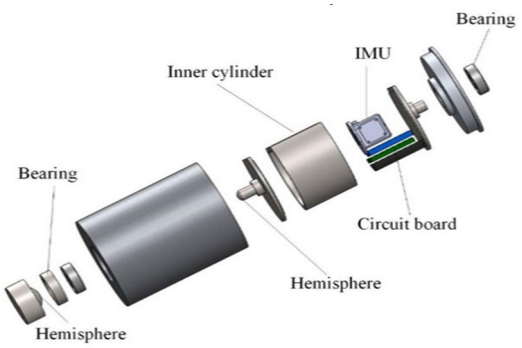

FIGURE 3. Exploded view of PSP.

A pair of alloy steel head-on hemispheres that can withstand overload during launch has been designed to improve the overload-burdening limit.

The head-on hemispheres were installed in the PSP on the side close to the projectile tail. This structure is used to protect the bearings to avoid damage during the launching process. The hemispheres collide on the top to prevent shock to the inner cylinder when the projectile is launching. The details of the two hemispheres are shown in Figure 4.

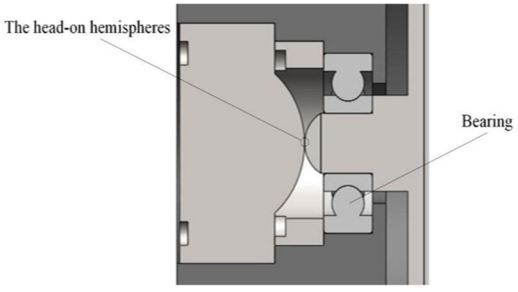

FIGURE 4. Two hemispheres.

IV. MODELLING AND SIMULATION OF PSP

The stability of the PSP largely determines the performance of the PSINS. A variety of factors may affect the stability of the PSP, such as the quality, rotary inertia, and mass eccentricity of the inner cylinder. In addition, the type of bearing and friction coefficient can also affect the PSP's stability. In addition, the lift, gravity, and thrust, as well as the change in the pitch angle and high-speed rolling motion, may also affect the movement of the PSP's inner cylinder.

A. MODELLING

Before modeling, it is assumed that the projectile has a short-range and small angle of attack and is flying at low altitude, with pitch and yaw angles changing at a low angular rate. Then, it can be confirmed that the force of gravity is constant, and the direction of drag is coincident with the longitudinal axis of the projectile. Figure 5 is the force diagram of the flying projectile; as shown, the projectile is subject to gravity, lift, drag, and thrust. The gravity is in the vertically downward direction, the lift is in the perpendicular projectile upward direction, the drag is in the direction opposite to the flight, and the thrust is in the direction of flight.

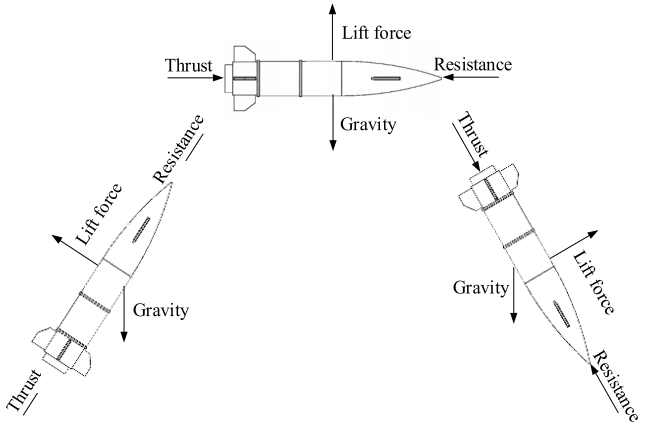

FIGURE 5. Force condition of flying projectile.

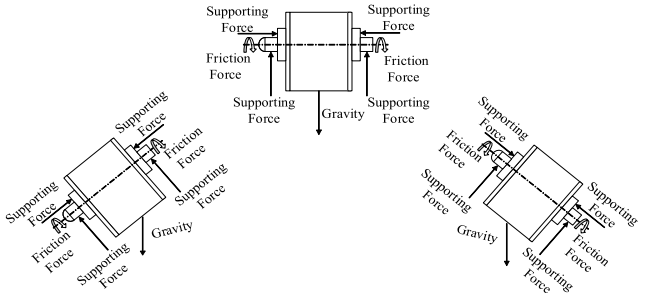

FIGURE 6. Force condition of PSP's inner cylinder.

The force condition of the PSP's inner cylinder is shown in Figure 6. The rolling movement of the projectile drives the bearings to rotate and produce frictional force. In the vertical direction, the inner cylinder is subject to gravity; in the radial direction, the inner cylinder is subject to supporting force from the deep groove ball bearing because the projectile is subject to the lift and thrust. In addition, in the axial direction, the inner cylinder is also subject to supporting the force from the deep groove ball bearing because the projectile is subject to thrust and drag.

Using the force condition of the PSP's inner cylinder, the mechanical model can be simplified as a compound pendulum installed inside the projectile, as shown in Figure 7. It is assumed that a_l is the acceleration of the projectile in the vertical direction. The compound pendulum swings oscillating around point O. Point C is the center of mass, $\theta(t)$ is the swing angle, and M_f is the friction torque. Gravity, mg, provides the pendulum with a restoring moment. The axial supporting force and radial supporting force act on point O in two different directions.

It should be noted that the PSP is not suited for projectiles that are launched vertically, in principle. If the pitch angle equals 90°, there is no force moment, and the PSP will not remain stable.

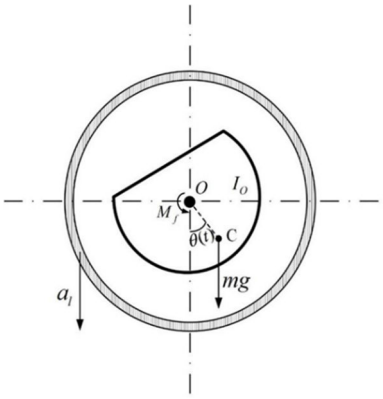

FIGURE 7. Simplified mechanical model.

B. DYNAMIC EQUATION

On the basis of the simplified mechanical model shown in Figure 7, it is assumed that M_O is the sum of external moments, M_f is the friction moment, and M_g (provided by mg) is the restoring moment. Then,

$$M_O = M_f - M_g \tag{1}$$

From Newton's second law of motion, the sum of external force moments is equal to the product of the rotational inertia and the angular acceleration along the fixed axis. Therefore, M_O can also be expressed as

$$M_O = I_O\ddot{\theta}(t) \tag{2}$$

where $\ddot{\theta}(t)$ is the angular acceleration. From (1) and (2), the initial dynamic equation can be obtained as

$$I_O\ddot{\theta}(t) - M_f + M_g = 0 \tag{3}$$

where M_g is determined by mg and a_l; mg is the force of gravity on the inner cylinder, and a_l is the projectile acceleration in the vertical direction. Moreover, $\alpha(t)$ is the pitch angle. Therefore, M_g can be defined as

$$M_g = m\,[g - a_l(t)]\sin\theta(t)\cdot l\cos\alpha(t) \tag{4}$$

where

$$a_l(t) = g - \frac{Y_s(t)}{M} = g - \frac{\rho V(t)^2 S C_y}{2M} \tag{5}$$

where

$$Y_s(t) = \frac{1}{2}\rho V(t)^2 S C_y \tag{6}$$

where $Y_s(t)$ is the lift force on the projectile, M is the total weight of the projectile, $V(t)$ is the flying speed, S is the reference area of the projectile, and C_y is the lift coefficient.

The friction moment M_f is determined by the type and loads of bearings, and bearing loads are determined by gravity mg and the supporting force of the inner cylinder. Bearing loads can be divided into the radial load F_r and axial load F_a,

$$F_r = m\,[g - a_l(t)]\cos\alpha(t) \tag{7}$$

$$F_a = m\,[g - a_l(t)]\sin\alpha(t) + ma_z(t) \tag{8}$$

where $a_z(t)$ is the acceleration produced by the integrative action of thrust and resistance.

$$a_z(t) = \frac{F + Y_z(t)}{M} \tag{9}$$

where

$$Y_z(t) = \frac{1}{2}\rho V(t)^2 S C_x \tag{10}$$

where F is thrust, $Y_z(t)$ is resistance, and C_x is the resistance coefficient.

A number of methods can be used to calculate the bearing friction moment. One of the most precise methods is provided by work [29]:

$$M_{skf} = M_{rr} + M_{sl} + M_{seal} + M_{drag} \tag{11}$$

where M_{skf} is the total frictional moment, M_{rr} is the rolling frictional moment, M_{sl} is the sliding frictional moment, M_{seal} is the frictional moment of the seal, and M_{drag} is the frictional moment from drag losses, churning, splashing.

TABLE 1. Parameter values for inner cylinder.

Symbol	Significance	Value	Unit
m	Quality	0.536	kg
I_0	Moment of inertia	0.0003359	$kg \bullet m^2$
l	Mass eccentricity	0.0021	m
g	Acceleration of gravity	9.8	$N\ /\ m^2$
M_{skf}	Friction torque	0.000366	$N \bullet m$

Finally, the ultimate dynamic equation is obtained as

$$I_O\ddot{\theta}(t) - M_{skf} + m\,[g - a_l(t)]\sin\theta(t)\cdot l\cos\alpha(t) = 0 \tag{12}$$

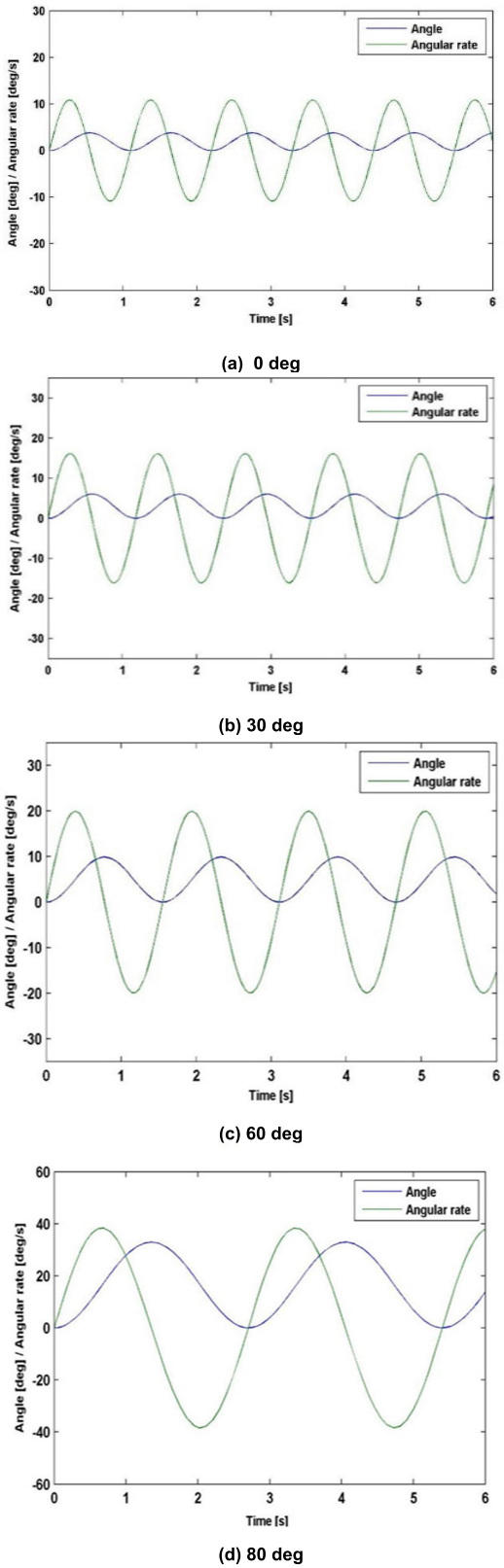

FIGURE 8. Angle and angular rate obtained from simulation.

C. SIMULATIONS

Simulations were conducted to verify the dynamic models and research the stability of the PSP. The parameters of a finished PSP are listed in Table 1, where $\boldsymbol{m}$, $\boldsymbol{I_0}$, and $\boldsymbol{l}$ are measured values, and the value of $\boldsymbol{M_{skf}}$ is obtained from calculations. $\boldsymbol{a_l(t)}$ is set to zero to contrast with the results of the ground turntable test later.

Inserting the data into (12), the following equation is obtained:

$$\ddot{\theta}(t) - 1.2896 + 45.7487 \cdot \sin\theta(t)\cos\alpha(t) = 0 \quad (13)$$

The above equation is a second-order non-homogeneous nonlinear ordinary differential equation. Setting the initial value of the equation as $\boldsymbol{\theta(0) = 0}$, $\boldsymbol{\dot{\theta}(0) = 0}$ and setting the projectile pitch angles $\boldsymbol{\alpha(t)}$ as 0°, 30°, 60°, and 80°, the fourth-order Runge-Kutta numerical integration method can be used to solve this equation in MATLAB (Version r2008a, The Mathworks Inc., USA). Eventually, the graph of the equation's solution $\boldsymbol{\theta(t)}$ and $\boldsymbol{\dot{\theta}\ (t)}$ was drawn up like Figure 8 ***(a)*** ∼ ***(d)***.

FIGURE 9. High-speed turntable.

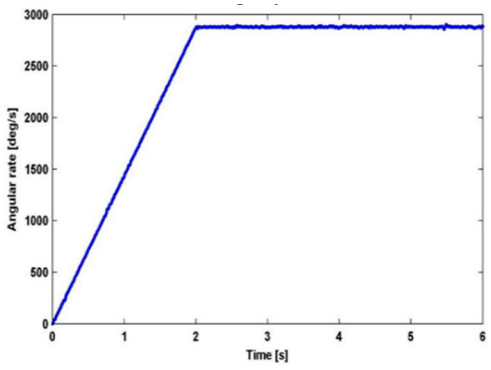

FIGURE 10. Angular rate for turntable roll axis.

The simulation results show that the inner cylinder undergoes swing movement under the assumed conditions. When $\boldsymbol{\alpha(t)}$ is taken to be 0°, the inner cylinder has the minimum swing angular rate and angle. With increasing $\boldsymbol{\alpha(t)}$, the angular swing rate and angle gradually increase, and the swing frequency is gradually reduced. When $\boldsymbol{\alpha(t)}$ reaches 80°, the angle rate is up to 40°/s.

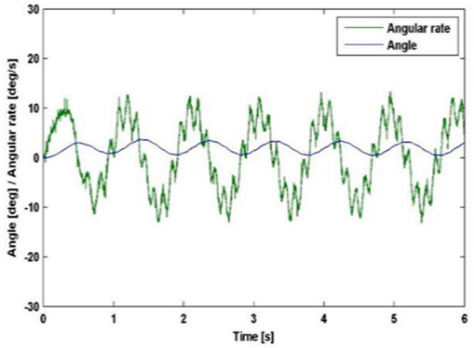

(a) 0 deg

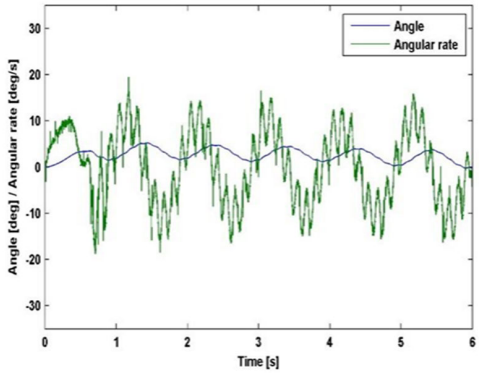

(b) 30 deg

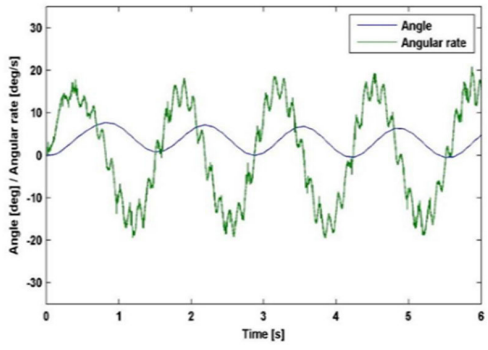

(c) 60 deg

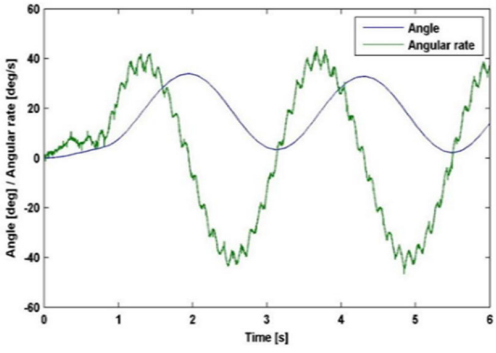

(d) 80 deg

FIGURE 11. Angle and angular rate test results.

V. GROUND TEST

Ground tests on a high-speed three-axis turntable were performed to verify the computer simulation results. The pitch angle of the turntable was set to 0°, 30°, 60°, and 80°, and the roll axis of the turntable was set to rotate at 2880°/s. Furthermore, the pitch axis and yaw axis were fixed as the roll axis was rotating. A Micro Electro Mechanical System (MEMS) gyroscope was installed in the roll axis of the cylinder to measure the movement of the PSP's inner cylinder. Figure 10 shows the rolling rate history of the turntable from the feedback data. Figure 11 ***(a)*** ∼ ***(d)*** show the rolling angular rate history of the PSP's inner cylinder.

(a)A 125 mm gun at test ground.

(b) Projectile wreckage. (c) Recovered PSP

FIGURE 12. Fire trial scene.

The results show that the PSP's inner cylinder was undergoing stable swing movement during the test. The inner cylinder had a minimum angular swing rate and angle when the pitch angle of the turntable was at 0°. With increasing pitch angle, the swing angular rate and angle gradually increased; meanwhile, the swing frequency was gradually reduced. The angular rate was up to 40°/s when the pitch angle reached 80°. Take the test results of Figure 11 ***(a)***∼ ***(d)*** comparing with the simulation results of Figure 8 ***(a)*** ∼ ***(d)***, it is very consistent about the swing period and amplitude.

Otherwise, the angular rates of test results had a slight oscillation with a frequency of 8 Hz. The effect contributing to this variation is the rolling frequency of the turntable. The roll axis of the turntable was set to rotate at 8 rpm in the test, and there are inevitable fixing errors between the PSP and

turntable. As a result, the oscillation of the test angular rates was produced.

VI. GUN FIRING TEST

Gun firing tests were performed to verify the overloading burdening and the stabilization function of the PSP. Two 125-mm gun-launched projectiles were fired during the tests. The launching over-loading in the tests is approximately 8000 g, and the projectiles typically roll at 14-20 Hz. Additionally, the angle of fire is +5°. The PSP was installed in the projectile. Figure 12 ***(a)*∼*(c)*** show the fire trial scene; it includes a 125 mm gun at test ground, a 125 mm gun launched projectile, projectile wreckage, and recovered PSP.

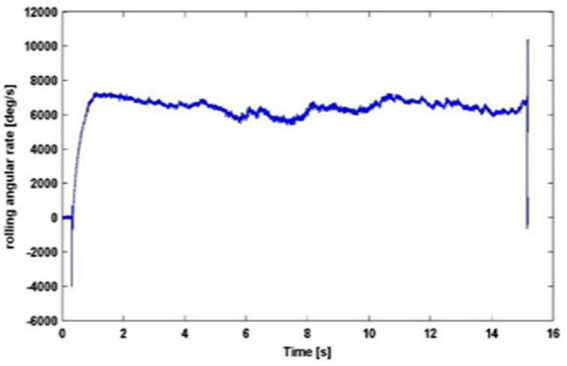

(a) The test angular rate of the projectile.

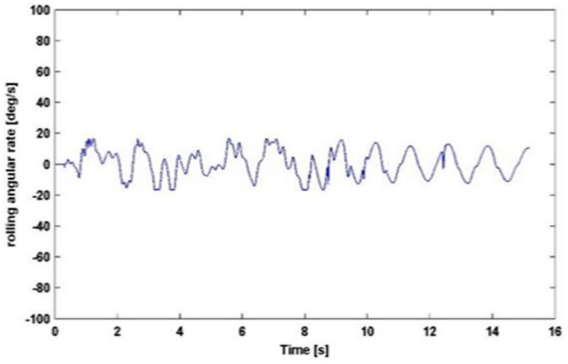

(b) The test angular rate of the PSP.

FIGURE 13. Roll rate obtained from sensors in PSP and projectile during flight.

The test results showed that the PSP survived an 8000 g launch and displayed stability during the flight. The angular rate history of one test projectile is shown in Figure 13(a); the rolling angular rate is measured by a MEMS gyroscope with its sense axis oriented perpendicular to the projectile's spin axis. The rolling angular rate of the projectile reached its maximum value within approximately 0.8 s of flight. The angular rate history of the PSP's inner cylinder applied in the above projectile is shown in Figure 13(b); another MEMS gyroscope was installed in the cylinder to make the measurement. The angular rate of the PSP's inner cylinder changed within the range of approximately ±20°/s. It indicated that the PSP's inner cylinder provided a relatively stable platform. Otherwise, there are certain differences between flight test results and simulation and ground test results, which include a smaller oscillation waveform and higher peak-to-peak value. Four effects contribute to this variation: the assumptions that were made in the computation simulation (such as that $\boldsymbol{M_{skf}}$ was assumed to be constant, and α(t) was assumed to discrete change), the shock and vibration, the change of airlift and drag, and the uncertainty relating to unknown atmospheric conditions (e.g., density). Despite these fluctuations, the PSP greatly reduced the high-speed rolling impact from the projectile.

VII. CONCLUSION

A novel partial strapdown navigation approach for a high G gun-launched rolling projectile was developed in this study. Appling the partial strapdown platform into the projectile, provided a marked stable effect. The harmful effects of high-speed rolling on the INS were reduced. The overload-burdening limit was improved by using a pair of specially designed head-on hemispheres. The INS can remain stable in the projectile roll axis direction while remaining strapdown in the pitch axis and yaw axis directions. The requirements for the gyroscope's measurement range are reduced; consequently, MEMS sensors, showing good overload performance, small size, and low cost, can be used to complete measurements in the PSINS. The stability of the PSP's inner cylinder is associated with the pitch angle. When the pitch angle is small, the PSP is more stable. These features of the PSP were verified through modeling, simulation, and turntable experiments. The overload-burdening and stabilization functions of the PSP were demonstrated through gun firing tests.

REFERENCES

[1] H. Ghanbarpourasl, "Attitude reconstruction from strap-down rate gyros using power series," *J. Navigat.*, vol. 74, no. 4, pp. 763–781, Jul. 2021.

[2] T. Zhang and X. Xu, "A new method of seamless land navigation for GPS/INS integrated system," *Measurement*, vol. 45, no. 4, pp. 691–701, 2012.

[3] R. Barrett-Gonzalez, R. Barnhart, and R. Bramlette, "Steerable adaptive bullet flight control mechanism design," in *Proc. 53rd AIAA/ASME/ASCE/AHS/ASC Struct., Struct. Dyn. Mater. Conf.*, Honolulu, HI, USA, Apr. 2012, p. 1511.

[4] F. Fresconi, "Guidance and control of a projectile with reduced sensor and actuator requirements," *J. Guid., Control, Dyn.*, vol. 34, no. 6, pp. 1757–1766, 2011.

[5] J. Niehus and C. Mracek, "Laser guided rocket inertial measurement unit performance determination using trajectory reconstruction," in *Proc. AIAA Guid., Navigat., Control Conf.*, Toronto, ON, Canada, Aug. 2010, p. 8323.

[6] P. Singh, M. Esposito, Z. Barrons, C. A. Clermont, J. Wannop, and D. Stefanyshyn, "Measuring gait velocity and stride length with an ultrawide bandwidth local positioning system and an inertial measurement unit," *Sensors*, vol. 21, no. 9, p. 2896, Apr. 2021.

[7] Y. Zhou, S. Lai, H. Cheng, A. H. M. Redhwan, P. Wang, J. Zhu, Z. Gao, Z. Ma, Y. Bi, F. Lin, and B. M. Chen, "Toward autonomy of micro aerial vehicles in unknown and global positioning system denied environments," *IEEE Trans. Ind. Electron.*, vol. 68, no. 8, pp. 7642–7651, Aug. 2021.

[8] S. H. Song, "H∞ approach to performance analysis of missile control systems with proportional navigation guidance laws," *J. Electr. Eng. Technol.*, vol. 16, no. 2, pp. 1083–1088, 2021.

[9] R. Glebocki and M. Zugaj, "Gasodynamic control system for INS guided bomb," in *Proc. 47th AIAA Aerosp. Sci. Meeting*, Orlando, FL, USA, Jan. 2009, p. 311.
[10] Q. Nie and X. Gao, "Comparison of nonlinear filtering approach in tightly-coupled GPS/INS navigation system," in *Proc. 10th World Congr. Intell. Control Autom. (WCICA)*, Jul. 2012, pp. 1176–1181.
[11] J. Rogers and M. Costello, "Smart projectile state estimation using evidence theory," *J. Guid., Control, Dyn.*, vol. 35, no. 3, pp. 824–833, May 2012.
[12] J. Connelly, A. Kourepenis, and T. Marinis, "Micromechanical sensors in tactical GN&C applications," in *Proc. AIAA Guid., Navigat., Control Conf.*, Denver, CO, USA, Aug. 2000, p. 4381.
[13] J.-W. Kim, H.-W. Kang, H.-C. Jeong, D.-H. Hwang, S.-J. Lee, T.-G. Lee, and K.-W. Song, "GPS/INS integrated navigation systems design for spinning smart munitions," *J. Korea Inst. Mil. Sci. Technol.*, vol. 12, no. 5, pp. 615–621, 2009.
[14] Q. Chen, Z. Wang, S. Chang, and J. Fu, "Multiphase trajectory optimization for gun-launched glide guided projectiles," *Proc. Inst. Mech. Eng. G, J. Aerosp. Eng.*, vol. 230, no. 6, pp. 995–1010, May 2016.
[15] L. Thomas and N. John, "International HARM precision navigation upgrade—A GPS/INS missile upgrade that improves effectiveness and minimizes friendly-fire accidents," *IEEE Aerosp. Electron. Syst. Mag.*, vol. 18, no. 5, pp. 26–31, May 2003.
[16] J. Wendel and G. F. Tromme, "Tightly coupled GPS/INS integration for missile applications," *Aerosp. Sci. Technol.*, vol. 8, no. 7, pp. 627–634, 2004.
[17] P. Rouger, "Guidance and control of artillery projectiles with magnetic sensors," in *Proc. 45th AIAA Aerosp. Sci. Meeting Exhibit*, Reno, NV, USA, Jan. 2007, p. 1203.
[18] E. Ohlmeyer, J. Fraysse, and T. Pepitone, "Guidance, navigation and control without gyros: A gun-launched munition concept," in *Proc. AIAA Guid., Navigat., Control Conf. Exhibit*, Monterey, CA, USA, Aug. 2002, p. 5025.
[19] M. Li, G. Dai, H. L. Tang, X. P. He, and B. Peng, "Realization of micro inertial measurement unit used in high dynamic environment," *J. Chin. Inertial Technol.*, vol. 20, no. 2, pp. 127–130, 2012.
[20] J. Wei, H. Li, T. Wang, and Y. Wang, "Research on the guidance technology of air-to-ship missile attacking nearshore ship," *J. Phys., Conf. Ser.*, vol. 1852, no. 3, Apr. 2021, Art. no. 032056.
[21] M. Bashir, S. A. Khan, L. Udayagiri, and A. Noor, "Dynamic stability of unguided projectile with 6-DOF trajectory modeling," in *Proc. 2nd Int. Conf. Converg. Technol. (I2CT)*, Apr. 2017, pp. 1002–1009.
[22] C. Murphy and W. Mermagen, "Flight mechanics of an elastic symmetric missile," *J. Guid. Control Dyn.*, vol. 24, no. 6, p. 76, 2000.
[23] C. Umstead, Y. Tay, and H. Lankarani, "Multibody modelling of an internal gyroscopic micro-mechanism for development of lateral deviation of a projectile," *Proc. Inst. Mech. Eng. K, J. Multi-Body Dyn.*, vol. 230, no. 3, pp. 226–236, Sep. 2016.
[24] G. Frost and G. Costello, "Control authority of a projectile equipped with an internal unbalanced part," *J. Dyn. Syst., Meas., Control*, vol. 128, no. 4, pp. 1005–1012, 2006.
[25] J. Rogers and M. Costello, "Control authority of a projectile equipped with a controllable internal translating mass," *J. Guid., Control, Dyn.*, vol. 31, no. 5, pp. 1323–1333, 2008.
[26] J. Rogers and M. Costello, "A variable stability projectile using an internal moving mass," *Proc. Inst. Mech. Eng. G, J. Aerosp. Eng.*, vol. 223, no. 7, pp. 927–938, Jul. 2009.
[27] X. Zhang, J. Li, L. P. Hou, J. D. Zhu, and L. Qin, "Analysis and compensation of installation axial angle errors of semi-strapdown IMS," *Acta Armamentarii*, vol. 36, no. 7, pp. 1222–1227, 2015.
[28] X. Wei, J. Li, T. Zheng, X. Zhang, K. Feng, and H. Qian, "Design of anti-high-overload structure of passive semi-strapdown stabilization platform," *Explosion Shock Waves*, vol. 39, no. 7, 2019, Art. no. 075102.
[29] SKF. (2013). *The SKF Model for Calculating the Frictional Moment*. Accessed: Dec. 20, 2013. [Online]. Available: http://www.skf.com/group/products/bearings-units-housings/ball-bearings/principles/friction/skf-model/index.html?WT.oss=Frictional%20moment&WT.z_oss_boost=0&tabname=All&WT.z_oss_rank=1

XIAO-MIN DUAN received the Ph.D. degree in instrument science and technology from the North University of China, Taiyuan, China, in 2015. He is currently a Postdoctoral Researcher with the School of Electronic Science and Engineering, University of Electronic Science and Technology of China, Chengdu, China. His research interest includes the fields of inertial sensors and systems.

HUILIANG CAO (Member, IEEE) received the Ph.D. degree in instrument science and technology from Southeast University, Nanjing, China, in 2014. From 2011 to 2012, he studied as a Research Ph.D. Student with the School of Electrical and Computer Engineering, Georgia Institute of Technology, Atlanta, USA. He is one of the Top Young Academic Leaders of Higher Learning Institutions of Shanxi and Young Academic Leaders of North University of China. He is currently a Postgraduate Tutor and an Associate Professor with the School of Instrument and Electronics, North University of China, Taiyuan, Shanxi, China. His research interest includes MEMS inertial devices.